ELSEVIER

Journal of Alloys and Compounds 408–412 (2006) 260–265

Journal of ALLOYS AND COMPOUNDS

www.elsevier.com/locate/jallcom

Development of high-coercivity nanocomposite permanent magnets based on $Nd_2Fe_{14}B$ and Fe_xB

Satoshi Hirosawa *, Hirokazu Kanekiyo, Toshio Miyoshi, Yasutaka Shigemoto, Kaichi Murakami, Yuuka Senzaki, Takashi Nishiuchi

Research and Development Center, NEOMAX Co., Ltd., 2-15-17 Egawa, Shimamoto-cho, Mishima-gun, Osaka-fu 618-0013, Japan

Available online 18 July 2005

Abstract

In a composition range along the tie line between Fe_3B and $Nd_2Fe_{14}B$ with Nd concentration between approximately 6 and 9 at%, it has been found that addition of a few atomic percent of Ti suppresses formation and growth of γ-iron and promotes the formation of $Nd_2Fe_{14}B$. This lead to development of a new series of nanocomposite permanent magnet materials on the Nd–Fe–B–Ti–C system, for which the strip-casting technique can be applied in the rapid solidification process. The newly developed Nd–Fe–B–Ti–C nanocomposite permanent magnets cover a wide range of magnetic properties and include a high-coercivity grade with coercivity (H_{cJ}) of about 1 MA/m and remanence (B_r) of 0.8 T and a high-remanence grade with H_{cJ} = 500 kA/m and B_r = 0.86 T. The high coercivity owes its origin to a larger volume fraction of the hard magnetic $Nd_2Fe_{14}B$ phase compared to the previous $Fe_3B/Nd_2Fe_{14}B$ nanocomposite permanent magnets in which the volume fraction of the $Nd_2Fe_{14}B$ phase is limited by disappearance of this phase in Nd concentration range beyond about 5 at%. Resin-bonded magnets fabricated using these powders show excellent stability against oxidation under a humid, high-temperature atmosphere.

Keywords: Nanocomposite; Permanent magnet; Rapid solidification; Neodimium–iron–boron

1. Introduction

Recent investigations have shown that, in a composition range along the tie line between Fe_3B and $Nd_2Fe_{14}B$ with Nd concentration between approximately 6 and 9 at%, addition of a few atomic percent of Ti suppresses formation and growth of γ-iron and promotes the formation of $Nd_2Fe_{14}B$ on the course of rapid solidification and that excellent nanocomposite permanent magnet materials can be obtained [1–3]. These investigations have also revealed that addition of a small amount of C refines the microstructure, which results in realization of a high coercivity. The excellent glass-forming ability of these alloys allows adoption of a high-throughput rapid solidification technique called "strip-casting" (SC), which has been used increasingly in production of high-end Nd–Fe–B sintered magnets [4]. SC is basically a process to obtain a continuous strip by extracting a molten alloy from a pool of liquid by using a moving surface of a chilled drum. Upon contact with the drum surface, the alloy quickly solidifies and is extracted from the melt pool as strips. The SC process differs from the melt-spinning process in that the molten alloys are simply poured upon a guide and lead to a chilled roll whereas in the MS process the alloys are ejected from a small orifice by applying pressure.

Together with the previously developed $Fe_3B/Nd_2Fe_{14}B$ nanocomposites with Cr–Co additions [5], the strip-castable nanocomposite permanent magnets now cover magnetic properties ranging from B_r = 0.92 T and H_{cJ} = 360 kA/m to B_r = 0.8 T and H_{cJ} = 1000 kA/m. This paper reports magnetic properties of the $Fe–B/Nd_2Fe_{14}B$-based nanocomposite permanent magnet powders produced by means of the strip-casting and a subsequent heat-treatment. Also reported are

* Corresponding author. Tel.: +81 75 961 5351; fax: +81 75 962 9690.
E-mail address: HIROSAWA.S@neomax.co.jp (S. Hirosawa).

0925-8388/$ – see front matter © 2005 Elsevier B.V. All rights reserved.
doi:10.1016/j.jallcom.2005.04.200

magnetic and other physical properties of their resin-bonded magnets.

2. Experimental procedures

For a preliminary research using the melt-spinning process, melt-spinning process using a Cu wheel was used. Phases existing in the melt-spun ribbons were identified with powder X-ray diffraction (XRD) technique using Cu Kα. Portions of the melt-spun ribbons were heat-treated in an argon atmosphere to generate hard magnetic properties. For the strip-casting experiments, a vacuum furnace equipped with a water-cooled Cu dram was used. The density of the flakes was determined to be 7.46 Mg/m^3 by means of the Archimedean method using relatively bulky nano-structured cast flakes produced by the casting apparatus. Magnetic properties of the ribbons were measured at room temperature with a vibrating sample magnetometer (VSM) after magnetizing the ribbons with a magnetic field of at least 3.2 MA/m. Resin-bonded magnets were produced by using an ordinary epoxy binder for the compression-molding and polyamide (Nylon-12) for the injection-molding processes.

3. Results

The phases observed by means of powder X-ray diffraction analysis on melt-spun flakes of Nd–Fe–B–Ti alloys are shown on (Fe–Ti)–Nd–B concentration maps in Fig. 1. In the as-spun state, the Nd-poor composition range of the ternary alloys contains α-Fe and $Nd_2Fe_{14}B$ crystalline phases and a small amount of an amorphous phase (not indicated in the figure) for V_s of 20 m/s (Fig. 1a). With 3 at% addition of Ti, which partially replaces Fe, formation of α-Fe (which is believed to be originally γ-Fe on crystallization and transformed on cooling to the α-Fe) and a significant amount of the amorphous phase remains with the primary crystals of $Nd_2Fe_{14}B$ (Fig. 1b) at the same V_s of 20 m/s. The excellent glass-forming ability of the B-rich Nd–Fe–B alloys is seen when V_s is lowered down to 10 m/s. In this condition, the alloys with 3 at% of Ti crystallizes into a mixture of Fe–B compounds and $Nd_2Fe_{14}B$ in the Nd-poor and B-rich composition range (Fig. 1c).

The effects of Ti and C on the phase formation behaviors in the B-rich and Nd-depleted composition range provides a possibility of applying the strip-casting process to produce nanocrystalline alloys for the $Fe_xB/Nd_2Fe_{14}B$ nanocomposite permanent magnets. Several alloys with different Nd concentrations ranging from 4.5 to 9 at% were processed into nanocomposite permanent magnets via the SC process. Typical average thickness of SC-processed flakes obtained in the present investigation ranged from about 70 to about 100 μm. Powder particles obtained by crushing annealed thick flakes have morphology quite different from a platelet morphology of powder particles produced by melt-spinning and pulverization. Fig. 2 compares the powder particle morphology of these powders.

Table 1 shows magnetic properties of $Fe_xB/Nd_2Fe_{14}B$-type nanocomposite hard magnetic powders obtained by means of strip-casting and annealing. A wide range of magnetic properties was generated by compositional modifications. Powder no. 1 is a Cr–Co-added $Fe_3B/Nd_2Fe_{14}B$-type and nos. 2–5 are the Nd–Fe–B–Ti–C-type nanocomposites. The intrinsic coercivity is governed principally by Nd content (see Table 1), being larger for the larger Nd content. This is reasonable because the larger Nd content leads to the larger volume fraction of the hard magnetic $Nd_2Fe_{14}B$ phase. The Fe–B phase in the alloy no. 1 with Nd content of about 4.5% is almost exclusively Fe_3B, whereas the crystallographic structure of the Fe–B phases in powders nos. 2–5 with Nd concentration ranging from about 6 at% (powder no. 2) to about 9 at% (powder no. 5) are expected to be one of or combination of Fe_2B, Fe_3B, and $Fe_{23}B_6$. Demagnetization curves of these powders are shown in Fig. 3.

The low concentration of rare earth elements in the powder provides better stability against an oxidizing atmosphere in comparison to conventional Nd–Fe–B powders with near-stroichimetric $Nd_2Fe_{14}B$ compositions. Fig. 4a shows demagnetisation curves of the Nd–Fe–B–Ti–C powder no. 4 after exposure to the ambient air at elevated temperatures for various duration of time. For comparison, demagnetisation curves of a conventional Nd–Fe–B powder (commercial

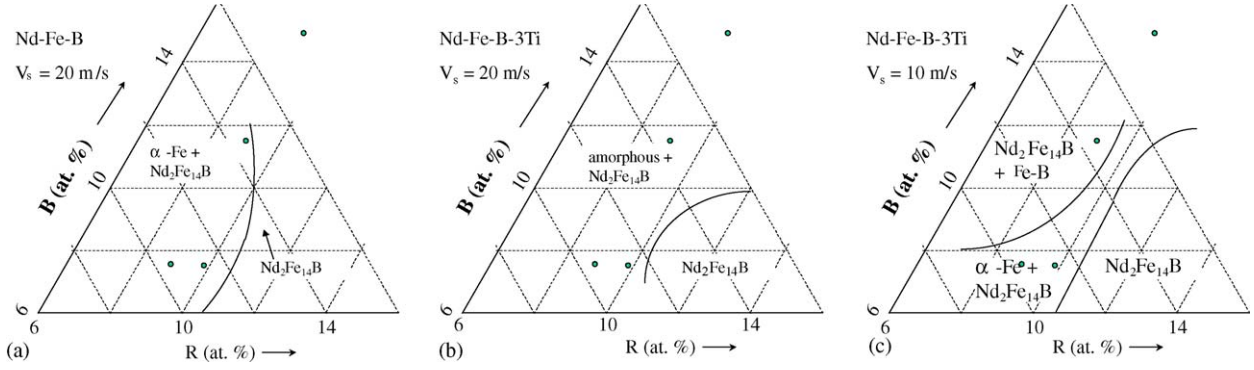

Fig. 1. Phases observed by means of powder X-ray diffraction analysis on melt-spun flakes of Nd–Fe–B–Ti alloys.

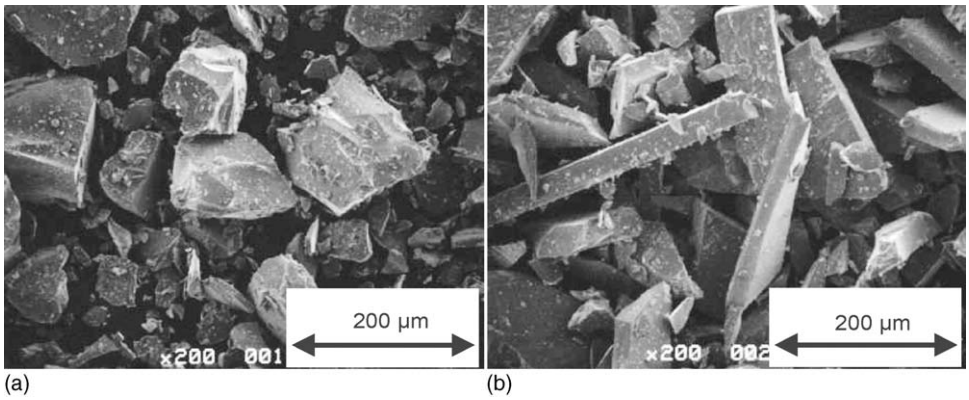

Fig. 2. Scanning electron microscopic images of pulverized powders of (a) a strip-cast Nd–Fe–B–Ti–C alloy and (b) a nearly single-phase $Nd_2Fe_{14}B$ melt-spun alloy.

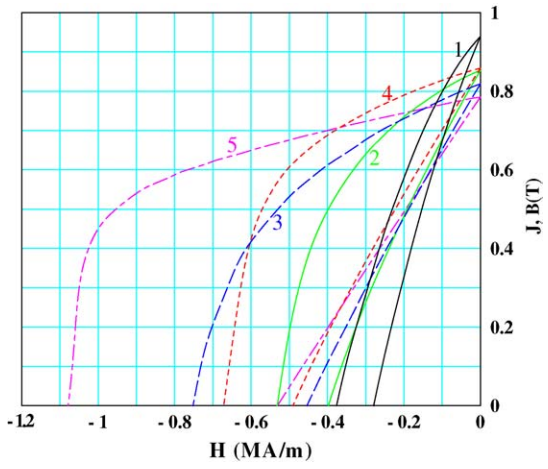

Fig. 3. Demagnetization curves of powders nos. 1–5 listed in Table 1.

grade MQP-O powder purchased from Magnequench International Corporation), after a similar oxidising test, are shown in Fig. 4b. This experiment suggests that the magnetic properties of the nanocomposite magnet are much insensitive to high temperature air in comparison to the conventional Nd–Fe–B powder, which showed marked breakdown of second quadrant demagnetisation curves. Therefore, the nanocomposite

Table 1
Typical magnetic properties of Fe–B/$Nd_2Fe_{14}B$ nanocomposite permanent magnet powders obtained via strip-casting

Powder no.	Type	Nd (at%)	B_r (T)	H_{cJ} (kA/m)	$(BH)_{max}$ (kJ/m^3)
1	Nd–Fe–B–Cr–Co	4.5	0.94	380	80
2	Nd–Fe–B–Ti–C	6	0.86	500	98
3	Nd–Fe–B–Ti–C	7	0.81	640	103
4	Nd–Fe–B–Ti–C	8.5	0.82	725	99
5	Nd–Fe–B–Ti–C	9	0.80	1000	104

powder is more suitable for the high temperature applications than the conventional type of powder.

The significant difference in the sensitivity to the high-temperature ambient environment may be attributed to the difference in sensitivity of the powder to oxygen. The Nd–Fe–B–Ti–C nanocomposite powder no. 4 and the conventional powder contain, respectively, approximately 7.5 and 12 at% Nd. Fig. 5a shows weight gain due to oxidation of the powders during exposure to the ambient air at elevated temperatures for ten minutes, as measured using a thermo-gravimetry. Above about 300 °C, there is a significant difference between these two kinds of powders in the oxygen pick-up, which is shown in Fig. 5b for the same powders as a function of temperature.

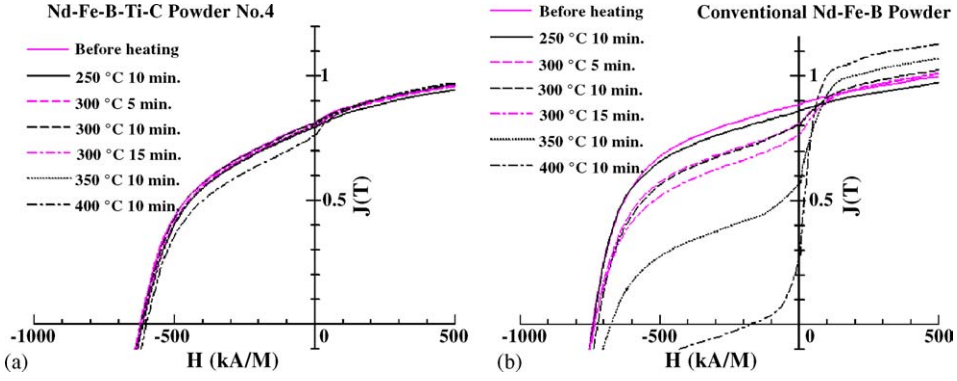

Fig. 4. Demagnetisation curves of the Nd–Fe–B–Ti–C powder no. 4 (left panel) and conventional Nd–Fe–B isotropic powder (right panel) after exposure to ambient air at elevated temperatures for various duration of time.

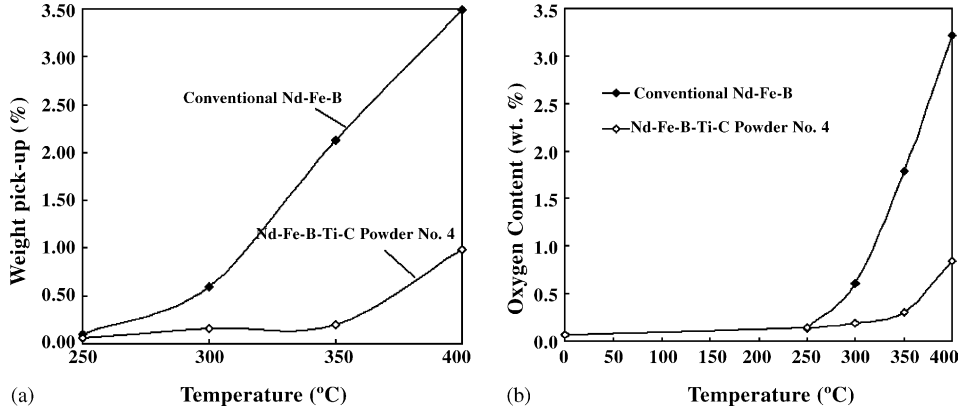

Fig. 5. Weight gain (a) and oxygen content (b) of powders during exposure to ambient air at elevated temperature for 10 min.

Magnetic properties of resin-bonded magnets of the powders shown in Table 1 are summarised in Table 2. These values are comparable to those obtained from conventional nearly single-phase $Nd_2Fe_{14}B$-based isotropic powders.

Fig. 6a and b show time dependence of flux losses for, respectively, compaction-molded magnets (with 2.5 wt% epoxy and with a permeance coefficient (P_c) of approximately 2) and injection-molded magnets with $P_c = 1$ under an 80 °C, 90 relative humidity air. The magnets were without surface coating and the result may be subject to sample preparation conditions such as selection of the resin and molding pressures. The larger initial thermal losses in the injection-molded magnets are due to the smaller P_c value of the specimens ($P_c = 1$) than the compression-molded specimens ($P_c = 2$). The decay of magnetic flux density after the initial loss is due to both the magnetic after effect and the structural losses. The former is also dependent on the H_{cJ} and P_c values, or more precisely on the irrevesible susceptibility at the operating line. The structural losses are material sensitive. The comparison between powder nos. 3 or 4 and MQP-B, an industrial standard material for Nd–Fe–B resin-bonded magnets, reveals that the nanocomposite powders with less Nd contents have better stability in the long-run exposure test.

The initial thermal losses are principally determined by the H_{cJ} and P_c values. The dependence of initial thermal losses of these compaction-molded magnets on temperature to which the magnets were exposed for 1 h are shown in Figs. 7 and 8

Table 2
Typical magnetic properties of resin-bonded magnets made of powders shown in Table 1

Molding process	Powder no.	Density (Mg/m^3)	B_r (T)	H_{cJ} (kA/m)	$(BH)_{max}$ (kJ/m^3)
Compaction	1	6.1	0.84	370	66
	2	6.1	0.70	500	69
	3	6.1	0.70	620	78
	4	6.1	0.67	725	72
	5	6.1	0.64	1000	67
Injection	1	5.2	0.60	345	38.2
	2	5.2	0.556	503	45.1
	3	5.1	0.546	625	46.9

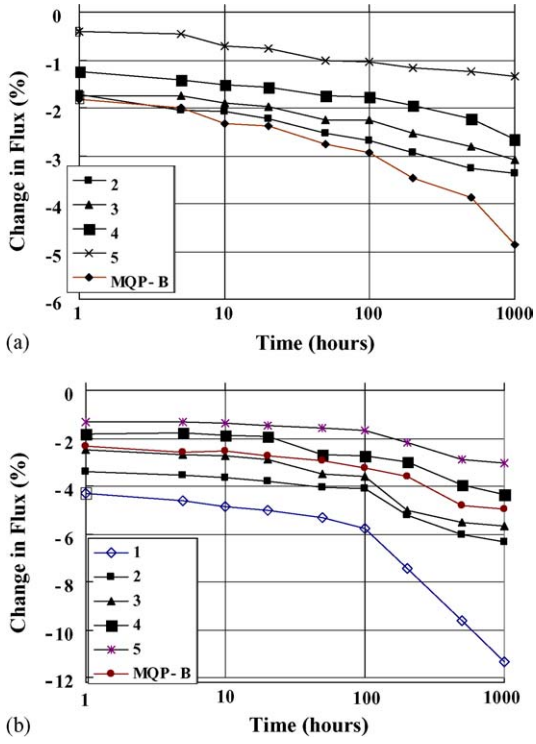

Fig. 6. Changes in magnetic flux in a 80 °C–90% RH exposure test for (a) compression-molded magnets with an outer diameter of 10 mm and a height of 7 mm ($P_c = 2$) and (b) injection-molded magnets with an outer diameter of 15 mm and a height of 5 mm ($P_c = 1$).

for, respectively, injection-molded $P_c = 1$ magnets with the polyamide binder and compression-molded $P_c = 2$ magnets with epoxy binder. The high coercivity powder (no. 5) shows excellent persistence up to high temperatures relevant even to automobile applications (160–200 °C).

4. Discussion

With addition of Ti, the primary formation of the γ-Fe was completely prevented from occurring for the cooling rates relevant to formation of the nanocomposite (Fig. 1b and c),

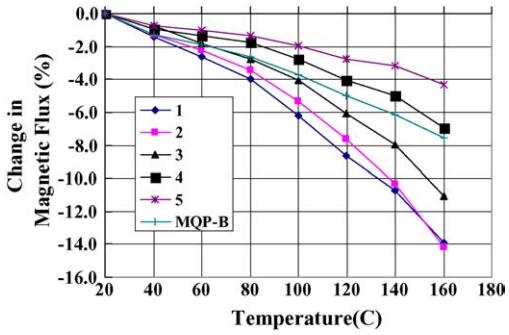

Fig. 7. Initial thermal flux losses of injection-molded resin-bonded magnets with a permeance coefficient of 1.

resulting in the direct formation of $Nd_2Fe_{14}B$ from the deeply under cooled liquid phase as the primary phase. The remaining liquid phase may either remain as an amorphous phase or crystallize into one of Fe–B compounds, such as Fe_2B, which may be taken over by metastable Fe_3B or $Fe_{23}B_6$ for higher cooling rates. In the subsequent annealing procedure, these grain boundary phases are transformed into a fully crystallized phase surrounding the $Nd_2Fe_{14}B$ crystals.

One of the implications that stems from this argument is the morphology of the nanocomposite structure that is created during rapid solidification. With the primary phase in the Nd–Fe–B–Ti system being $Nd_2Fe_{14}B$, the remainder crystallizes as intergranular phase in a thin, film-like morphology [1–3]. This is in a sharp contrast to the previously developed $Fe_3B/Nd_2Fe_{14}B$-type alloys, which are prepared from an amorphous phase via primary crystallization of Fe_3B and subsequent crystallization of $Nd_2Fe_{14}B$ [5,6]. For hard magnetic properties, the interior volumes of the magnetically softer phase should be within the exchange correlation length $L_{ex} = (A/\mu_0 M_s^2)^{1/2}$; the length scale over which the ferromagnetic coupling overwhelms static magnetic interactions (A is exchange stiffness and M_s is saturation magnetic moment). Values of L_{ex} are about 2–3 nm for ferromagnetic phases of large magnetization with typical values for A = 8–10 pJ/m and $\mu_0 M_s$ = 1.6–2 T. The previous high-resolution transmission

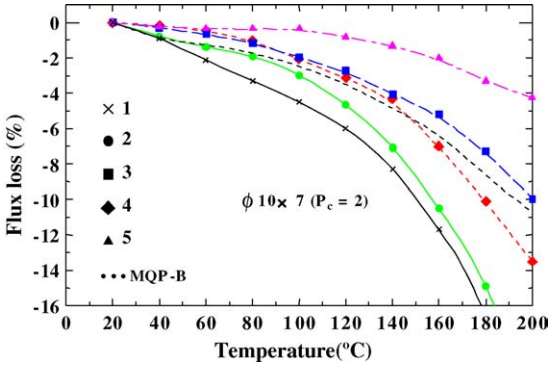

Fig. 8. Initial thermal flux losses of compaction-molded resin-bonded magnets with a permeance coefficient of 2.

electron microscopic investigation revealed that the thickness of the Fe–B intergranular phases is around 5 nm or smaller, which is suitable for generation of a high coercivity according to the above-mentioned argument. This microstructure is also favorable for obtaining good corrosion resistance.

Being strip-castable for preparation of rapidly-solidified precursor alloy production, the Nd–Fe–B–Ti–C alloys have practical impacts as a hard magnetic powder for making isotropic resin-bonded magnets. First of all, the powder can be produced in an industrial scale with a far greater throughput in comparison to the conventional Nd–Fe–B powders, which are produced by means of the melt-spinning process. After the preparation of the rapidly solidified precursor alloys, they are simply heat-treated and pulverized to be used as the hard magnetic powder for production of the resin-bonded magnets.

Secondly, the low rare-earth concentrations in the powder and aforementioned microstructure of the Nd–Fe–B–Ti–C nanocomposites have provided greater stability against hot ambient air and a highly humid environment in comparison to the conventional Nd–Fe–B powders with near-stroichimetric $Nd_2Fe_{14}B$ compositions particularly above about 300 °C. These characteristics of the Nd–Fe–B–Ti–C powders may make them unique for production of thermo-plastic compounds for the injection-molding process particularly when resins with high melting temperatures such as polyphenylene sulfide (PPS) resins or liquid crystal polymers are used.

Thirdly, the particle shape of ground powders of the strip-cast nanocomposites is brick-like, quite different from the flaky shape of conventional Nd–Fe–B powders. This difference arises from the difference in thickness of the original rapidly solidified alloys, which stems from the large difference in the glass-forming ability of each alloys system. Generally, particles with aspect ratio close to unity are more suitable to obtain high melt flow rates in compounds for the injection molding process than the flaky one, although compound compositions and kneading conditions are sometimes also important to this property. A high melt flow is essential to assure successful injection of the thermally plastic compound into narrow or thin cavities.

For the commercial applications, the isotropic nanocomposite permanent magnets have entered to the stage of industrial utilization as a hard magnetic ingredient for resin-bonded magnets and may penetrate into various application areas of resin-bonded magnets.

5. Conclusion

It was shown that, in a composition range along the tie line between Fe_3B and $Nd_2Fe_{14}B$ with Nd concentration, a new series of nanocomposite permanent magnet powders can be produced on the Nd–Fe–B–Ti–C-based alloy system. The newly developed Nd–Fe–B–Ti–C nanocomposite permanent magnets cover a wide range of magnetic prop-

erties and include a high-coercivity grade with coercivity (H_{cJ}) of about 1 MA/m and remanence (B_r) of 0.8 T and a high-remanence grade with $H_{cJ} = 500$ kA/m and $B_r = 0.86$ T for which the strip-casting process is used for the production of rapidly solidified precursor alloys. Together with the previously developed $Fe_3B/Nd_2Fe_{14}B$-type nanocomposites, the strip-castable nanocomposite permanent magnets now cover magnetic ranging from $B_r = 0.92$ T, $H_{cJ} = 360$ kA/m to $B_r = 0.8$ T, $H_{cJ} = 1000$ kA/m. The low rare earth content of these nanocomposite magnets provides good resistance against ambient air at high temperatures and highly humid environments, assuring a high stability of magnetic properties of resin-bonded magnets in such environments. These alloys may be used as hard magnetic powders for isotropic resin-bonded magnets. The high-temperature stability and the brick-like powder morphology may make these powders unique candidates for various applications.

References

[1] S. Hirosawa, H. Kanekiyo, Y. Shigemoto, T. Miyoshi, J. Jpn. Soc. Powder Powder Metall. 51 (143) (2004) (in Japanese).
[2] S. Hirosawa, H. Kanekiyo, T. Miyoshi, J. Magn. Magn. Mater. 281 (2004) 58.
[3] S. Hirosawa, H. Kanekiyo, T. Miyoshi, K. Murakimi, T. Shigemoto, T. Nishiuchi, IEEE Trans. Magn. 40 (4) (2004) 2883.
[4] J. Bernardi, J. Fidler, M. Sagawa, Y. Hirose, J. Appl. Phys. 83 (1998) 6396.
[5] H. Kanekiyo, S. Hirosawa, J. Appl. Phys. 83 (11) (1998) 6265.
[6] S. Hirosawa, H. Kanekiyo, Y. Shigemoto, MRS Symp. Proc. 577 (1999) 141.